 CMES, vol.87, no.1, pp.1-22, 2012

An Improved Numerical Evaluation Scheme of the Fundamental Solution and its Derivatives for 3D Anisotropic Elasticity Based on Fourier Series

Y.C. Shiah[1], C. L. Tan[2] and C.Y. Wang[1]

Abstract: The fundamental solution, or Green's function, for 3D anisotropic elastostatics as derived by Ting and Lee (1997) [Q.J. Mech. Appl. Math.; 50: 407-426] is one that is fully explicit and algebraic in form. It has, however, only been utilized in boundary element method (BEM) formulations quite recently even though it is relatively straightforward and direct to implement. This Green's function and its derivatives are necessary items in this numerical analysis technique. By virtue of the periodic nature of the angles when it is expressed in the spherical coordinate system, the present authors have very recently represented the Green's function as a double Fourier series for their efficient numerical evaluation. The Fourier coefficients are determined only once, independent of the total number of field points involved in the BEM analysis of a problem. The derivatives of the fundamental solution can also be obtained simply by direct spatial differentiation of the double Fourier series without further numerical or significant analytical steps. This paper presents a re-formulation of the same scheme by taking advantage of some characteristic features of the Fourier coefficients and re-arranging and simplifying the terms. In so doing, the total number of terms necessary for the series summation is significantly reduced thereby enhancing further its computational efficiency, especially when large number of field points are involved as is typically the case when modeling practical engineering problems. Numerical examples are presented to demonstrate the veracity of the proposed scheme. It is also simpler to implement into BEM codes because of the formulation is considerably less elaborate as compared to the direct evaluation approaches of the exact analytical solution, its full explicit algebraic form notwithstanding.

Keywords: Boundary element method, Green's functions, boundary integral equations, anisotropic elasticity, Stroh's eigenvalues, Fourier series.

[1] Dept. of Aerospace and Systems Engineering, Feng Chia University, Taichung, Taiwan, R.O.C.
[2] Dept. of Mechanical & Aerospace Engineering, Carleton University, Ottawa, Canada K1S 5B6

1 Introduction

The fundamental solution or Green's function to the governing differential equation of the physical problem and its derivatives are essential items in the direct formulation of the boundary element method (BEM) and some meshless methods. In elastic stress analysis, the Green's function for displacements and its first derivatives are used in the derivation of the conventional displacement-boundary integral equation (BIE); higher order derivatives of this fundamental solution are required for evaluating the stresses at interior points via Somigliana's identity, and in, e.g., the formulation of the traction-BIE. The fundamental solution for displacements in a 3D generally anisotropic solid that was first derived by Lifschitz and Rozentsweig (1947) was not of closed-form and is expressed as a line integral around a unit circle. Over the past few decades, much attention has been devoted to simplifying the line integral into more explicit analytical forms as well as on the development of efficient algorithms for their accurate and stable numerical evaluation. The papers by, for example, Barnett (1972), Wilson and Cruse (1978), Schlar (1994), Gray *et al* (1996), Wang (1997), Sales (1998), Tonon *et al* (2001), Phan *et al* (2004), Wang and Denda (2007), Tavara *et al* (2008), Shiah and Tan (2008), Tan *et al* (2009) and Buroni and Saez (2010) provide a selection of these works using the various approaches and in the context of BEM development; a more extensive review is given in, e.g. Tan and Shiah (2009), Shiah *et al* (2010).

Ting and Lee (1997) and Lee (2003) have also derived an algebraic, real variable form of the Green's function for displacements and its derivatives in a 3D generally anisotropic solid, respectively. They are expressed in terms of Stroh's eigenvalues. The explicit forms of these fundamental solutions make their implementation into existing BEM codes relatively simpler as compared to previous ones. This was, however, only recognized quite recently; its introduction into BEM formulations was first carried out by Tavara *et al* (2008) for the special case of transverse isotropy, and by the present lead authors for full general anisotropy (Shiah *et al* (2008), Tan *et al* (2009)), as well as by Buroni and Saez (2010). The BEM implementation in these latter three papers, although fairly straightforward, revealed the disproportionate amount of computational effort taken in evaluating higher order derivatives of the fundamental solution because of the presence of very high order tensor terms (up to 10^{th} order for 2^{nd} order derivatives). This prompted Lee (2009) to re-examine the problem and new general forms of the Green's function derivatives, expressed in terms of spherical coordinates, were obtained without the very high order tensor terms present. Using this revised approach and the residue theorem for high-order poles, the lead authors derived the explicit algebraic expressions of the 1^{st} and 2^{nd} order derivatives, and implemented them in the BEM for computing internal point stresses in 3D generally anisotropic solids recently (Shiah *et al*

(2010)), demonstrating too (Shiah *et al* (2011, 2012)) the better computational performance, typically by a factor of about 2 for practical problems over the previous formulation. These explicit forms of the derivatives are, however, rather lengthy and tedious; their implementation, although still relatively straightforward, is quite involved. It can be expected that this will be more so for even higher-order derivatives of the Green function that are required in, for example, hyper-singular BEM formulations.

An alternative approach to evaluate Ting and Lee's (1997) fundamental solution and its derivatives was proposed by the present authors very recently in Shiah *et al* (2012). It is recognized that the angles in the spherical coordinate system used in Ting and Lee's solution are periodic. For the purpose of numerical evaluation, the Green's function can thus be represented by a double Fourier series. The Fourier coefficients are numerically determined, and this is done only once irrespective of the number of field points in the numerical solution domain. The derivatives of the fundamental solution are obtained by direct spatial differentiation on the Fourier series. The implementation of this approach into the BEM code for the computation of the fundamental solution and its derivatives is considerably less elaborate. In that study, it is also shown that very significant savings in computer CPU time is achieved without, for all intents and purposes, any sacrifice on the numerical accuracy. This makes the scheme a very attractive efficient alternative for practical engineering problems as the number of field points at which the fundamental solution and its derivatives are required is very large indeed, typically in the order of 10^6 or higher.

The present study deals with an extension of the work reported in Shiah *et al* (2012). In this paper, advantage is taken of some characteristic features of the Fourier coefficients, thereby re-formulating some of the expressions for the series summation. By doing so, it will be shown that further increase in efficiency of the computational effort to compute the fundamental solution and its derivatives can be achieved. The veracity of the numerical values obtained are demonstrated by examples in which the quantities are obtained at some sample field points and compared with the exact values calculated using the previous direct approaches of Shiah *et al* (2008), Tan *et al* (2009), hereinafter referred to as Approach 1; and Shiah *et al* (2010, 2011), hereafter referred to as Approach 2. Ways to overcome the numerical singularity that can occur for some very special cases are also discussed. The relative CPU run times for evaluating the fundamental solution and its first and second derivatives using the present Fourier series scheme and those presented in Shiah *et al* (2012) are then compared for increasing number of field points. First, however, a brief review of the fundamental solution of Ting and Lee (1997) is in order.

2 Fundamental solution for displacements

The fundamental solution in elastostatics, $U_{ij}(P,Q) \equiv \mathbf{U(x)}$, is defined as the displacement in the x_i-direction at the field point Q due to a unit load applied in the x_j-direction at P in a homogeneous infinite elastic solid. That for 3D general anisotropic elasticity as derived by Ting and Lee (1997) is of a fully explicit, algebraic form, unlike those derived by others previously. It can be expressed in simple closed-form as

$$\mathbf{U}(\mathbf{x}) = \frac{1}{4\pi r}\mathbf{H}[\mathbf{x}], \tag{1a}$$

or, in spherical coordinates, as

$$\mathbf{U}(r,\theta,\phi) = \frac{\mathbf{H}(\theta,\phi)}{4\pi r}, \tag{1b}$$

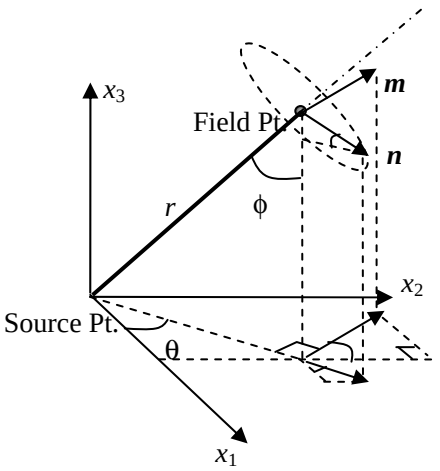

Figure 1: Unit circle, $|\mathbf{n}^*| = 1$, on the oblique plane at the field point.

In Eq. (1), r is the radial distance between the load point and field point, and $\mathbf{H}(\theta,\phi)$, the Barnett-Lothe tensor, depends only on the spherical angles (θ, ϕ) defined in the usual sense, as shown in Figure 1. With reference to this figure, the vectors **n**, **m** along with $\mathbf{n}^* \equiv \mathbf{x}/r$ form a right-handed triad [**n**, **m**, **x** / r]. The general form of **n** and **m** can be expressed as

$$\begin{aligned} \mathbf{n} &= (\cos\phi\cos\theta,\ \cos\phi\sin\theta,\ -\sin\phi), \\ \mathbf{m} &= (-\sin\theta,\ \cos\theta,\ 0), \end{aligned} \tag{2}$$

where $0 \leq \theta < 2\pi$ and $0 \leq \phi \leq \pi$.

The Barnett-Lothe tensor can be expressed in terms of Stroh's eigenvalues as

$$\mathbf{H}(\theta,\phi) = \frac{1}{|\boldsymbol{\kappa}|} \sum_{n=0}^{4} q_n \hat{\boldsymbol{\Gamma}}^{(n)}, \tag{3}$$

where the explicit expressions for q_n, $\hat{\boldsymbol{\Gamma}}^{(n)}$, and $\boldsymbol{\kappa}$ are given by

$$q_n = \begin{cases} \frac{-1}{2\beta_1\beta_2\beta_3}\left[Re\left\{\sum_{t=1}^{3}\frac{p_t^n}{(p_t-\bar{p}_{t+1})(p_t-\bar{p}_{t+2})}\right\} - \delta_{n2}\right] & \text{for } n = 0,1,2, \\ \frac{1}{2\beta_1\beta_2\beta_3} Re\left\{\sum_{t=1}^{3}\frac{p_t^{n-2}\bar{p}_{t+1}\bar{p}_{t+2}}{(p_t-\bar{p}_{t+1})(p_t-\bar{p}_{t+2})}\right\} & \text{for } n = 3,\ 4, \end{cases} \tag{4a}$$

$$\hat{\Gamma}_{ij}^{(n)} = \tilde{\Gamma}_{(i+1)(j+1)(i+2)(j+2)}^{(n)} - \tilde{\Gamma}_{(i+1)(j+2)(i+2)(j+1)}^{(n)}, \quad (i,j = 1,\ 2,\ 3), \tag{4b}$$

$$\boldsymbol{\kappa} \equiv \kappa_{ik} = C_{ijks} m_j m_s \tag{4c}$$

where C_{ijks} are the elastic stiffness tensor of the anisotropic material and $\hat{\boldsymbol{\Gamma}}^{(n)}$ is the adjoint of the matrix $\boldsymbol{\Gamma}(p)$ defined as

$$\boldsymbol{\Gamma}(p) = \mathbf{Q} + p\mathbf{V} + p^2\boldsymbol{\kappa} \tag{5}$$

where

$$\mathbf{V} = (\mathbf{R} + \mathbf{R}^T) \tag{6}$$

and

$$Q \equiv Q_{ik} = C_{ijks} n_j n_s,\ R \equiv R_{ik} = C_{ijks} n_j m_s. \tag{7}$$

In Eq. (4a), the Stroh eigenvalues, p_i, are the roots of the sextic equation, namely, $|\Gamma(p)| = 0$. They are complex for positive strain energy and appear as three pairs of complex conjugates; these quantities can be expressed as

$$p_\nu = \alpha_\nu + \mathbf{i}\beta_\nu,\ \beta_\nu > 0,\ (\nu = 1,\ 2,\ 3) \tag{8}$$

with $\mathbf{i} = \sqrt{(-1)}$, and the overbar on p_i denoting the corresponding conjugate. With some basic algebraic manipulation, the tensor $\tilde{\boldsymbol{\Gamma}}^{(n)}$ can be shown to be

$$\begin{aligned} \tilde{\Gamma}_{pqrs}^{(4)} &= \kappa_{pq}\kappa_{rs}, \\ \tilde{\Gamma}_{pqrs}^{(3)} &= V_{pq}\kappa_{rs} + \kappa_{pq}V_{rs}, \\ \tilde{\Gamma}_{pqrs}^{(2)} &= \kappa_{pq}Q_{rs} + \kappa_{rs}Q_{pq} + \mathrm{V}_{pq}V_{rs}, \\ \tilde{\Gamma}_{pqrs}^{(1)} &= V_{pq}Q_{rs} + \mathrm{V}_{rs}Q_{pq}, \\ \tilde{\Gamma}_{pqrs}^{(0)} &= Q_{pq}Q_{rs}. \end{aligned} \tag{9}$$

With the explicit expressions presented above, it is evident that the calculations involved for obtaining the numerical value of **U(x)** are relatively straightforward. The only numerical scheme required in any of the above steps is to obtain the roots of the sextic equation for the Stroh's eigenvalues.

3 Fourier-series representations of U and its derivatives

Instead of computing the Bartnett-Lothe tensor, $\mathbf{H}[\mathbf{x}] \equiv \mathbf{H}(\theta, \phi)$, directly, the present authors have very recently proposed that it be represented by a double Fourier series (Shiah *et al* (2012)). It offers an efficient alternative for its numerical evaluation when the number of field points is very large, as is typically the case in practical engineering problems. Writing this tensor in the spherical coordinate system, the Fourier series representation may be expressed as follows,

$$H_{uv}(\theta,\phi) = \sum_{m=-\alpha}^{\alpha} \sum_{n=-\alpha}^{\alpha} \lambda_{uv}^{(m,n)}\, e^{i(m\theta+n\phi)}, \quad (u,\, v = 1,\, 2,\, 3), \tag{10}$$

where α is an integer large enough to ensure convergence of the series; $\lambda_{uv}^{(m,n)}$ are unknown coefficients to be determined. This is feasible because the tensor is periodic with an interval width 2π, that is,

$$H_{uv}(\theta,\, \phi + 2\pi) = H_{uv}(\theta,\, \phi) \tag{11}$$

The Fourier coefficients, $\lambda_{uv}^{(m,n)}$ are determined, from the theory of Fourier series, by

$$\lambda_{uv}^{(m,n)} = \frac{1}{4\pi^2} \int_{-\pi}^{\pi} \int_{-\pi}^{\pi} H_{uv}(\theta,\phi)\; e^{-i(m\theta+n\phi)} d\theta\, d\phi. \tag{12}$$

The integrals in Eq. (12) can be numerically evaluated. For example, if Gaussian quadrature is employed, Eq. (12) may be rewritten as

$$\lambda_{uv}^{(m,n)} = \frac{1}{4} \sum_{p=1}^{k} \sum_{q=1}^{k} w_p w_q f_{uv}^{(m,n)}(\pi\xi_p,\, \pi\xi_q), \tag{13}$$

where k is the number of the Gauss abscissa ξ_p, and w_p is the corresponding weight; $f_{uv}^{(m,n)}(\theta,\, \phi)$ represents the integrand in Eq.(12). Each computation of $\lambda_{uv}^{(m,n)}$ requires the evaluation of $H_{uv}(\theta,\phi)$ at the k^2 number of points,$(\pi\xi_p, \pi\xi_q)$, with Eqs.(4)-(9). For large values of m and n as are typically required in practice, the rapid fluctuations of $f_{uv}^{(m,n)}(\theta,\, \phi)$ as shown in Shiah *et al* (2012) makes it usually

necessary to use a relatively large number of Gauss points (typically greater than 30) to accurately perform the numerical integrations; k= 64 was used in that study and will be used here as well. Since the computational evaluation of the Fourier coefficients by Eq. (13) is carried out only once irrespective of the number of field points in an engineering analysis, the CPU time for this process is relatively small in comparison with computing directly Eq. (1) for every field point in the same BEM analysis of the problem.

The above numerical scheme in Shiah *et al* (2012) can be made even more efficient, as follows. When summing up the series terms, one can take advantage of the fact that, in Eq.(12), $\lambda_{uv}^{(m,n)}$ and $\lambda_{uv}^{(-m,-n)}$ are complex conjugates, i.e.

$$\lambda_{uv}^{(-m,-n)} = \overline{\lambda}_{uv}^{(m,n)}. \tag{14}$$

Let $\lambda_{uv}^{(m,n)}$ be separated into the real part $R_{uv}^{(m,n)}$ and the imaginary part $I_{uv}^{(m,n)}$ as shown below,

$$\lambda_{uv}^{(m,n)} = R_{uv}^{(m,n)} + \mathbf{i} I_{uv}^{(m,n)}. \tag{15}$$

As the imaginary part of $H_{uv}(\theta,\phi)$ must vanish, Eq.(10) can be rewritten as

$$H_{uv}(\theta,\phi) = \sum_{m=-\alpha}^{\alpha} \sum_{n=-\alpha}^{\alpha} h_{uv}^{(m,n)}(\theta,\phi), \tag{16}$$

where $h_{uv}^{(m,n)}(\theta,\phi)$ is defined by

$$h_{uv}^{(m,n)}(\theta,\phi) = R_{uv}^{(m,n)} \cos(m\theta + n\phi) - I_{uv}^{(m,n)} \sin(m\theta + n\phi). \tag{17}$$

By invoking Eq.(14), Eq. (16) above can be further simplified into

$$\begin{aligned} H_{uv}(\theta,\phi) = 2 \sum_{m=1}^{\alpha} \left\{ \sum_{n=1}^{\alpha} h_{uv}^{(m,n)}(\theta,\phi) + \sum_{n=-\alpha}^{-1} h_{uv}^{(m,n)}(\theta,\phi) \right\} \\ + 2 \sum_{n=1}^{\alpha} h_{uv}^{(0,n)}(\theta,\phi) + 2 \sum_{m=1}^{\alpha} h_{uv}^{(m,0)}(\theta,\phi) + R_{uv}^{(0,0)} \end{aligned}. \tag{18}$$

Substituting Eq. (17) into Eq. (18) and then into Eq. (1b), the fundamental solution **U** can now expressed as

$$U_{uv} = \frac{1}{2\pi r} \left\{ \begin{array}{l} \sum\limits_{m=1}^{\alpha} \sum\limits_{n=1}^{\alpha} \left[\begin{array}{l} \left(\tilde{R}_{uv}^{(m,n)} \cos m\theta - \tilde{I}_{uv}^{(m,n)} \sin m\theta \right) \cos n\phi \\ - \left(\hat{R}_{uv}^{(m,n)} \sin m\theta + \hat{I}_{uv}^{(m,n)} \cos m\theta \right) \sin n\phi \end{array} \right] \\ + \sum\limits_{m=1}^{\alpha} \left(\begin{array}{l} R_{uv}^{(0,m)} \cos m\phi - I_{uv}^{(0,m)} \sin m\phi \\ + R_{uv}^{(m,0)} \cos m\theta - I_{uv}^{(m,0)} \sin m\theta \end{array} \right) + \frac{R_{uv}^{(0,0)}}{2} \end{array} \right\}, \tag{19}$$

where $\tilde{R}_{uv}^{(m,n)}$, $\hat{R}_{uv}^{(m,n)}$, $\tilde{I}_{uv}^{(m,n)}$, and $\hat{I}_{uv}^{(m,n)}$ are given by

$$\begin{aligned} \tilde{R}_{uv}^{(m,n)} &= R_{uv}^{(m,n)} + R_{uv}^{(m,-n)}, \quad \hat{R}_{uv}^{(m,n)} = R_{uv}^{(m,n)} - R_{uv}^{(m,-n)}, \\ \tilde{I}_{uv}^{(m,n)} &= I_{uv}^{(m,n)} + I_{uv}^{(m,-n)}, \quad \hat{I}_{uv}^{(m,n)} = I_{uv}^{(m,n)} - I_{uv}^{(m,-n)}. \end{aligned} \tag{20}$$

It is worth noting that no operations of complex numbers are involved when evaluating **U** with Eq. (19). As the number of terms in the series has been reduced, this equation, being just as straightforward in form, is thus more efficient to use for the computations than the original formulation with Eqs. (10-13) reported in Shiah *et al* (012).

For the first and second order derivatives of **U**, as denoted here by for **U'** and **U''**, respectively, the steps involved and the exact explicit algebraic expressions obtained from the differentiation of Eq. (1) have been presented by Lee (2003, 2009) and Shiah *et al* (2008, 2010). Instead of using these exact analytical expressions, the present authors have shown that the derivatives can be accurately determined as well from direct spatial differentiations of Eq. (10) (Shiah *et al* (2012)). However, from the above re-formulation of the Fourier series summation, it can be expected that the same spatial differentiation will yield expressions that are more computationally efficient to evaluate too. Using the chain rule, the 1^{st}-order derivatives of the Green's function may be obtained from the following operation,

$$\text{U'} \equiv U_{uv,l} = \frac{\partial U_{uv}}{\partial r}\frac{\partial r}{\partial x_l} + \frac{\partial U_{uv}}{\partial \theta}\frac{\partial \theta}{\partial x_l} + \frac{\partial U_{uv}}{\partial \phi}\frac{\partial \phi}{\partial x_l}. \tag{21}$$

Let $\omega_l(\theta,\phi)$, $\omega_l'(\theta,\phi)$, and $\omega_l''(\theta,\phi)$ represent spatial differentiations defined as follows:

$$\omega_l(\theta,\phi) = r\frac{\partial r}{\partial x_l} = \begin{cases} \sin\phi\cos\theta, & (\text{for } l=1) \\ \sin\phi\sin\theta, & (for\ l=2) \\ \cos\phi, & (for\ l=3) \end{cases} \tag{22a}$$

$$\omega_l'(\theta,\phi) = r\frac{\partial \theta}{\partial x_l} = \begin{cases} -\sin\theta/\sin\phi, & (\text{for } l=1) \\ \cos\theta/\sin\phi, & (\text{for } l=2) \\ 0, & (\text{for } l=3) \end{cases} \tag{22b}$$

$$\omega_l''(\theta,\phi) = r\frac{\partial \phi}{\partial x_l} = \begin{cases} \cos\phi\cos\theta, & (\text{for } l=1) \\ \cos\phi\sin\theta, & (\text{for } l=2) \\ -\sin\phi, & (\text{for } l=3) \end{cases} \tag{22c}$$

Direct partial differentiation of **U** with respect to the spherical coordinates and using Eq. (21) would yield the following, as shown in Shiah *et al* (2012),

$$U_{uv,l} = \frac{1}{4\pi r^2}\begin{cases} \sum_{m=-\alpha}^{\alpha}\sum_{n=-\alpha}^{\alpha}\lambda_{uv}^{(m,n)}e^{\mathbf{i}(m\theta+n\phi)}\begin{bmatrix} -\cos\theta\ (\sin\phi-\mathbf{i}n\ \cos\phi) \\ -\mathbf{i}m\ \sin\theta/\sin\phi \end{bmatrix} & \text{for } l=1 \\ \sum_{m=-\alpha}^{\alpha}\sum_{n=-\alpha}^{\alpha}\lambda_{uv}^{(m,n)}e^{\mathbf{i}(m\theta+n\phi)}\begin{bmatrix} -\sin\theta\ (\sin\phi-\ \mathbf{i}n\ \cos\phi) \\ +\mathbf{i}m\ \cos\theta/\sin\phi \end{bmatrix} & \text{for } l=2\ \cdot \\ \sum_{m=-\alpha}^{\alpha}\sum_{n=-\alpha}^{\alpha}\lambda_{uv}^{(m,n)}e^{\mathbf{i}(m\theta+n\phi)}\left[-(\cos\phi+\mathbf{i}\,n\ \sin\phi)\right] & \text{for } l=3 \end{cases} \tag{23}$$

One may however use Eq.(19) instead for the differentiations; this will result in the following,

$$U_{uv,l} = \frac{1}{2\pi r^2}\left\{\begin{array}{l} -\omega_l(\theta,\phi)\left[\begin{array}{l}\sum_{m=1}^{\alpha}\sum_{n=1}^{\alpha}\left(\overleftarrow{\Gamma}_{uv}^{(m,n)}(\theta)\cos n\phi-\overrightarrow{\Gamma}_{uv}^{(m,n)}(\theta)\sin n\phi\right) \\ +\sum_{m=1}^{\alpha}(\overline{\gamma}_{uv}^{m}(\theta)+\check{\gamma}_{uv}^{m}(\phi))+\frac{R_{uv}^{(0,0)}}{2}\end{array}\right] \\ -\omega_l'(\theta,\phi)\left[\begin{array}{l}\sum_{m=1}^{\alpha}\sum_{n=1}^{\alpha}m\left(\tilde{\Gamma}_{uv}^{(m,n)}(\theta)\cos n\phi+\hat{\Gamma}_{uv}^{(m,n)}(\theta)\sin n\phi\right) \\ +\sum_{m=1}^{\alpha}m\cdot\tilde{\gamma}_{uv}^{m}(\theta)\end{array}\right] \\ -\omega_l''(\theta,\phi)\left[\begin{array}{l}\sum_{m=1}^{\alpha}\sum_{n=1}^{\alpha}n\left(\overleftarrow{\Gamma}_{uv}^{(m,n)}(\theta)\sin n\phi+\overrightarrow{\Gamma}_{uv}^{(m,n)}(\theta)\cos n\phi\right) \\ +\sum_{m=1}^{\alpha}m\cdot\hat{\gamma}_{uv}^{m}(\phi)\end{array}\right] \end{array}\right\}, \tag{24}$$

where

$$\begin{aligned} &\overleftarrow{\Gamma}_{uv}^{(m,n)}(\theta)=\tilde{R}_{uv}^{(m,n)}\cos m\theta-\tilde{I}_{uv}^{(m,n)}\sin m\theta,\quad \overrightarrow{\Gamma}_{uv}^{(m,n)}(\theta)=\hat{R}_{uv}^{(m,n)}\sin m\theta+\hat{I}_{uv}^{(m,n)}\cos m\theta, \\ &\tilde{\Gamma}_{uv}^{(m,n)}(\theta)=\tilde{R}_{uv}^{(m,n)}\sin m\theta+\tilde{I}_{uv}^{(m,n)}\cos m\theta,\quad \hat{\Gamma}_{uv}^{(m,n)}(\theta)=\hat{R}_{uv}^{(m,n)}\cos m\theta-\hat{I}_{uv}^{(m,n)}\sin m\theta, \\ &\overline{\gamma}_{uv}^{m}(\theta)=R_{uv}^{(m,0)}\cos m\,\theta-I_{uv}^{(m,0)}\sin m\,\theta,\quad \check{\gamma}_{uv}^{m}(\phi)=R_{uv}^{(0,m)}\cos m\phi-\ I_{uv}^{(0,m)}\sin m\phi, \\ &\tilde{\gamma}_{uv}^{m}(\theta)=R_{uv}^{(m,0)}\sin m\,\theta+I_{uv}^{(m,0)}\cos m\,\theta,\quad \hat{\gamma}_{uv}^{m}(\phi)=R_{uv}^{(0,m)}\sin m\,\phi+\ I_{uv}^{(0,m)}\cos m\,\phi. \end{aligned} \tag{25}$$

It should be noted that in Eq.(24), ω_l, ω_l', and ω_l'' are factors of the Fourier series sums; their evaluations are carried out only once for each of the field points. Although Eq. (24) may appear more elaborate in form than the original Fourier series

form of Eq. (23), it is structurally formulated to offer better efficiency in the summation process. This is evident from the reduction in the number of terms in the series summation and the absence of inter-linked algebraic operations. In practice too, a very significant number of the calculated coefficients are, for all intents and purposes, zero. The terms associated with them can therefore be skipped, thereby further reducing the processing time of the calculations.

There is the possibility of numerical singularity for $\mathbf{U}^{'}$ at $\phi = 0$ and $\phi = \pi$ that needs to be addressed. These conditions correspond to cases where the load and field points are both on the x_3-axis. As has been discussed in Shiah *et al* (2012), this is due to the fact that the spherical angle θ and its derivative at these locations become multi-valued and are ill-defined for l=1 and l=2. This problem may be easily resolved by introducing a small perturbation for ϕ, say ϕ= 10^{-6}, and selecting $\theta = 0$ for $l = 1$ (i.e. $\omega_1'(\theta,\phi) = 0$) and $\theta = \pi/2$ for $l = 2$ (i.e. $\omega_2'(\theta,\phi) = 0$). For convenience, $\theta = 0$ can be selected for l=3. Since all the calculations involved can be carried out by directly substituting the proper angular values in eq.(24), no explicit expression for this special case is presented here.

In the same manner, the 2^{nd}-order derivatives of $\mathbf{U}$ can be derived by directly taking differentiations of $\mathbf{U}^{'}$ in the spherical coordinates as follows:

$$U_{uv,lk} = \frac{\partial U_{uv,l}}{\partial r}\frac{\partial r}{\partial x_k} + \frac{\partial U_{uv,l}}{\partial \theta}\frac{\partial \theta}{\partial x_k} + \frac{\partial U_{uv,l}}{\partial \phi}\frac{\partial \phi}{\partial x_k}. \tag{26}$$

By taking differentiations of Eq. (23) and substituting it in Eq.(26), Shiah *et al* (2012) have derived the expressions for the six components of $\mathbf{U}''$, they are not presented here. In the present work, the 2^{nd}-order derivatives are alternatively obtained by differentiating Eq.(24) instead in the spherical coordinate system. With this, and following some re-arrangement of the various algebraic terms, the 2^{nd}-

order derivatives are expressed as

$$U_{uv,lk} = \frac{1}{2\pi r^3} \left\{ \begin{array}{c} \Omega_{lk}^{(1)}(\theta,\phi)\left[\sum_{m=1}^{\alpha}\sum_{n=1}^{\alpha}\tilde{\Lambda}_{uv}^{(m,n)}(\theta,\phi)+\sum_{m=1}^{\alpha}(\hat{\gamma}_{uv}^{m}(\theta)+\check{\gamma}_{uv}^{m}(\phi))+\frac{R_{uv}^{(0,0)}}{2}\right] \\ +\Omega_{lk}^{(2)}(\theta,\phi)\left[\sum_{m=1}^{\alpha}\sum_{n=1}^{\alpha} m\left(\tilde{\Gamma}_{uv}^{(m,n)}(\theta)\cos n\phi+\hat{\Gamma}_{uv}^{(m,n)}(\theta)\sin n\phi\right)+\sum_{m=1}^{\alpha} m\,\bar{\gamma}_{uv}^{m}(\theta)\right] \\ +\Omega_{lk}^{(3)}(\theta,\phi)\left[\sum_{m=1}^{\alpha}\sum_{n=1}^{\alpha} n\left(\overleftarrow{\Gamma}_{uv}^{(m,n)}(\theta)\sin n\phi+\overrightarrow{\Gamma}_{uv}^{(m,n)}(\theta)\cos n\phi\right)+\sum_{m=1}^{\alpha} m\,\hat{\gamma}_{uv}^{m}(\phi)\right] \\ +\Omega_{lk}^{(4)}(\theta,\phi)\sum_{m=1}^{\alpha}\sum_{n=1}^{\alpha} mn\left(\tilde{\Gamma}_{uv}^{(m,n)}(\theta)\sin n\phi-\hat{\Gamma}_{uv}^{(m,n)}(\theta)\cos n\phi\right) \\ +\Omega_{lk}^{(5)}(\theta,\phi)\left(\sum_{m=1}^{\alpha}\sum_{n=1}^{\alpha} m^2\tilde{\Lambda}_{uv}^{(m,n)}(\theta,\phi)+\sum_{m=1}^{\alpha} m^2\bar{\gamma}_{uv}^{m}(\theta)\right) \\ +\Omega_{lk}^{(6)}(\theta,\phi)\left(\sum_{m=1}^{\alpha}\sum_{n=1}^{\alpha} n^2\tilde{\Lambda}_{uv}^{(m,n)}(\theta,\phi)+\sum_{m=1}^{\alpha} m^2\check{\gamma}_{uv}^{m}(\phi)\right) \end{array} \right\}, \tag{27}$$

where the function $\tilde{\Lambda}_{uv}^{(m,n)}$, repeatedly appearing in the series, is defined as

$$\tilde{\Lambda}_{uv}^{(m,n)}(\theta,\phi) = \left(\overleftarrow{\Gamma}_{uv}^{(m,n)}(\theta)\cos n\phi - \overrightarrow{\Gamma}_{uv}^{(m,n)}(\theta)\sin n\phi\right), \tag{28}$$

and the other angular functions are defined as

$$\begin{aligned}
\Omega_{lk}^{(1)}(\theta,\phi) &= 2\omega_l(\theta,\phi)\omega_k(\theta,\phi) - \frac{\partial\omega_l(\theta,\phi)}{\partial\theta}\omega_k'(\theta,\phi) - \frac{\partial\omega_l(\theta,\phi)}{\partial\phi}\omega_k''(\theta,\phi), \\
\Omega_{lk}^{(2)}(\theta,\phi) &= 2\omega_l'(\theta,\phi)\omega_k(\theta,\phi) + \left(\omega_l(\theta,\phi) - \frac{\partial\omega_l'(\theta,\phi)}{\partial\theta}\right)\omega_k'(\theta,\phi) \\
&\quad - \frac{\partial\omega_l'(\theta,\phi)}{\partial\phi}\omega_k''(\theta,\phi), \\
\Omega_{lk}^{(3)}(\theta,\phi) &= 2\omega_l''(\theta,\phi)\omega_k(\theta,\phi) - \frac{\partial\omega_l''(\theta,\phi)}{\partial\theta}\omega_k'(\theta,\phi) \\
&\quad + \left(\omega_l(\theta,\phi) - \frac{\partial\omega_l''(\theta,\phi)}{\partial\phi}\right)\omega_k''(\theta,\phi), \\
\Omega_{lk}^{(4)}(\theta,\phi) &= \omega_l''(\theta,\phi)\,\omega_k'(\theta,\phi) + \omega_l'(\theta,\phi)\omega_k''(\theta,\phi), \\
\Omega_{lk}^{(5)}(\theta,\phi) &= -\omega_l'(\theta,\phi)\,\omega_k'(\theta,\phi), \\
\Omega_{lk}^{(6)}(\theta,\phi) &= -\omega_l''(\theta,\phi)\omega_k''(\theta,\phi).
\end{aligned} \tag{29}$$

It is worth pointing out that the angular functions $\Omega_{lk}^{(1)}(\theta,\phi) \sim \Omega_{lk}^{(6)}(\theta,\phi)$ in Eq. (29), which are symmetrical about (l, k), are all independent of m, n; thus, they need be computed only once for each of the field points. Substituting Eqs. (22a-c) into Eq.(29), they can be explicitly expressed as

$$\Omega_{lk}^{(1)}(\theta,\phi) = \begin{cases} 1.5\,(1-\cos 2\phi)\cos^2\theta - 1, & (l,k=1,1) \\ 1.5\sin 2\theta \sin^2\phi, & (l,k=1,2) \\ 1.5\cos\theta \sin 2\phi, & (l,k=1,3) \\ 1.5\,(1-\cos 2\phi)\sin^2\theta - 1, & (l,k=2,2) \\ 1.5\sin\theta \sin 2\phi, & (l,k=2,3) \\ 1.5\cos 2\phi + 0.5, & (l,k=3,3) \end{cases} \tag{30a}$$

$$\Omega_{lk}^{(2)}(\theta,\phi) = \begin{cases} -\sin 2\theta(1+1/\sin^2\phi), & (l,k=1,1) \\ \cos 2\theta(1+1/\sin^2\phi), & (l,k=1,2) \\ -\sin\theta\cot\phi, & (l,k=1,3) \\ \sin 2\theta(1+1/\sin^2\phi), & (l,k=2,2) \\ \cos\theta\cot\phi, & (l,k=2,3) \\ 0, & (l,k=3,3) \end{cases} \tag{30b}$$

$$\Omega_{lk}^{(3)}(\theta,\phi) = \begin{cases} 2\cos^2\theta\sin 2\phi - \sin^2\theta\cot\phi, & (l,k=1,1) \\ \sin 2\theta\,(0.5\cot\phi + \sin 2\phi), & (l,k=1,2) \\ 2\cos\theta\cos 2\phi, & (l,k=1,3) \\ 2\sin^2\theta\sin 2\phi - \cos^2\theta\cot\phi, & (l,k=2,2) \\ 2\sin\theta\cos 2\phi, & (l,k=2,3) \\ -2\sin 2\phi, & (l,k=3,3) \end{cases} \tag{30c}$$

$$\Omega_{lk}^{(4)}(\theta,\phi) = \begin{cases} -\sin 2\theta\cot\phi, & (l,k=1,1) \\ \cos 2\theta\cot\phi, & (l,k=1,2) \\ \sin\theta, & (l,k=1,3) \\ \sin 2\theta\cot\phi, & (l,k=2,2) \\ -\cos\theta, & (l,k=2,3) \\ 0, & (l,k=3,3) \end{cases} \tag{30d}$$

$$\Omega_{lk}^{(5)}(\theta,\phi)=\begin{cases}-\sin^2\theta/\sin^2\phi, & (l,k=1,1)\\ 0.5\sin 2\theta/\sin^2\phi, & (l,k=1,2)\\ 0, & (l,k=1,3)\\ -\cos^2\theta/\sin^2\phi, & (l,k=2,2)\\ 0, & (l,k=2,3)\\ 0, & (l,k=3,3)\end{cases} \tag{30e}$$

$$\Omega_{lk}^{(6)}(\theta,\phi)=\begin{cases}-\cos^2\theta\cos^2\phi, & (l,k=1,1)\\ -0.5\sin 2\theta\cos^2\phi, & (l,k=1,2)\\ 0.5\cos\theta\sin 2\phi, & (l,k=1,3)\\ -\sin^2\theta\cos^2\phi, & (l,k=2,2)\\ 0.5\sin\theta\sin 2\phi, & (l,k=2,3)\\ -\sin^2\phi, & (l,k=3,3)\end{cases} \tag{30f}$$

It is evident that in Eqs. (19), (24), and (27), there are numerous common terms appearing in the series; they require once-only calculation for a field point. In addition, all algebraic operations independent of *m*,*n* have been completely separated from the series. Although the original Fourier series formulations are more compact in the analytical form, their computations require more algebraic operations than this revised formulation.

The same numerical singularity issue exists for the condition when the load and field points simultaneously lie along the x_3-axis for the 2^{nd} order derivatives, except $U_{ij,33}$. As proposed by Shiah et al (2012), this problem can be easily overcome by the re-definition of the coordinates as shown in Fig. 2. For a point P on the x_3-axis, the corresponding $\hat{\phi}$ is defined by $\pi/2$; for the other angle, $\hat{\theta}=-\pi/2$ and $\hat{\theta}=\pi/2$ are used for x_3<0 and x_3>0, respectively. For these situations, the constitutive equation of generally anisotropic elasticity in the original Cartesian system, namely,

$$\begin{pmatrix}\sigma_{11}\\ \sigma_{22}\\ \sigma_{33}\\ \sigma_{23}\\ \sigma_{13}\\ \sigma_{12}\end{pmatrix}=\begin{pmatrix}C_{11} & C_{12} & C_{13} & C_{14} & C_{15} & C_{16}\\ C_{21} & C_{22} & C_{23} & C_{24} & C_{25} & C_{26}\\ C_{31} & C_{32} & C_{33} & C_{34} & C_{35} & C_{36}\\ C_{41} & C_{42} & C_{43} & C_{44} & C_{45} & C_{46}\\ C_{51} & C_{52} & C_{53} & C_{54} & C_{55} & C_{56}\\ C_{61} & C_{62} & C_{63} & C_{64} & C_{65} & C_{66}\end{pmatrix}\begin{pmatrix}\varepsilon_{11}\\ \varepsilon_{22}\\ \varepsilon_{33}\\ 2\varepsilon_{23}\\ 2\varepsilon_{13}\\ 2\varepsilon_{12}\end{pmatrix}, \tag{31}$$

where σ_{ij} and ε_{ij} represent the stresses and strains, respectively, needs to be transformed into the rotated coordinate system. The transformed stiffness coefficients

$\bar{C}_{ij}$ are given by

$$\bar{C}_{22}=C_{11},\ \bar{C}_{23}=C_{12},\ \bar{C}_{21}=C_{13},\ \bar{C}_{25}=C_{14},\ \bar{C}_{26}=C_{15},\ \bar{C}_{24}=C_{16},$$

$$\bar{C}_{33}=C_{22},\ \bar{C}_{31}=C_{23},\ \bar{C}_{35}=C_{24},\ \bar{C}_{36}=C_{25},\ \bar{C}_{34}=C_{26},\ \bar{C}_{11}=C_{33},$$

$$\bar{C}_{15}=C_{34},\ \bar{C}_{16}=C_{35},\ \bar{C}_{14}=C_{36},\ \bar{C}_{55}=C_{44},\ \bar{C}_{56}=C_{45},\ \bar{C}_{54}=C_{46},$$

$$\bar{C}_{66}=C_{55},\ \bar{C}_{64}=C_{56},\ \bar{C}_{44}=C_{66}. \tag{32}$$

Performing the Fourier series analysis with the re-defined stiffness coefficients gives the corresponding Fourier coefficients $\hat{\lambda}_{uv}^{(m,n)}$. The values of $\mathbf{U}^{"}$ for this case can then be obtained via the following substitutions:

$$U_{11,12}=\bar{U}_{33,13},\quad U_{12,12}=\bar{U}_{13,13},\quad U_{13,12}=\bar{U}_{23,13},$$

$$U_{22,12}=\bar{U}_{11,13},\quad U_{23,12}=\bar{U}_{12,13},\quad U_{33,12}=\bar{U}_{22,13}, \tag{33}$$

where $\bar{U}_{ij,mn}$ denotes the 2^{nd} order derivatives defined in the rotated coordinate system. Since the computations of the Fourier coefficients in this rotated system need to be performed only once if it ever arises in practice, this process is thus a trivial matter in terms of overall CPU time in a BEM analysis. It should also be reminded that in conventional displacement-BEM analysis, $\mathbf{U}''$ are only required when the stresses at internal points of the domain are required. Also this numerical singularity problem arises only when the internal point of interest is located exactly at the same (x_1, x_2) coordinates of any of the Gauss integration field points.

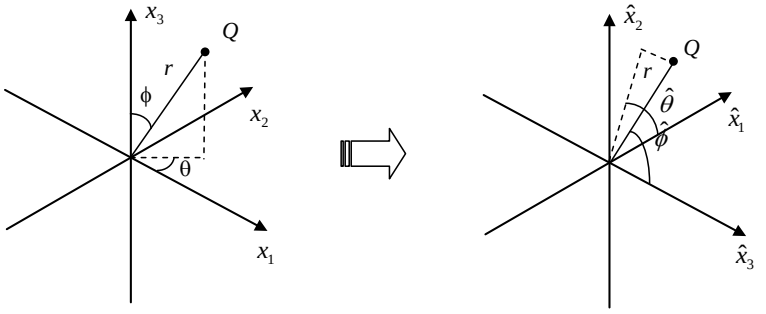

Figure 2: Spherical coordinates for (a) the original domain, and (b) the transformed domain

4 Numerical Examples

Some examples are presented here to demonstrate the veracity of the revised Fourier series scheme for the numerical evaluation of the fundamental solution **U** and its derivatives. Numerical values of **U**, $\mathbf{U}^{'}$ and $\mathbf{U}^{"}$ are obtained for some arbitrary field points in an anisotropic medium; their accuracy can be checked with those calculated from the corresponding exact solutions using two direct approaches, namely, Approach 1, as reported in Shiah *et al* (2008) and Tan *et al* (2009); and Approach 2 of Shiah *et al* (2010, 2011). As has been mentioned earlier, the CPU time involved in carrying out an engineering analysis using Approach 2 is typically half that of using Approach 1. The present authors have already shown, however, that the original Fourier series scheme is significantly more computationally efficient than these two approaches, besides its even simpler and easier implementation into a BEM code, Shiah *et al* (2012). This is particularly true when there are a large number of field points. It should be reminded that the present revised Fourier scheme presented in Section 3 is analytically equivalent to the original scheme and thus should produce identical numbers; it has just been re-formulated to take advantage of some of the features of the series to enhance the computer run-times. This superior CPU performance over the original Fourier series scheme will be demonstrated here as well.

For the numerical tests, the material chosen is Al_2O_3 crystal which has the following non-zero stiffness coefficients (Huntington (1958)):

$$C_{11} = 465GPa,\ C_{33} = 563GPa,\ C_{44} = 233GPa,$$
$$C_{12} = 124GPa,\ C_{13} = 117GPa,\ C_{14} = 101GPa. \tag{34}$$

As a demonstration of the present scheme to treat full anisotropy, the principal material axes in the x_1-, x_2- and x_3-directions of the alumina are arbitrarily rotated clockwise in sequence by 15^o, 30^o and 70^o, respectively. The resulting fully populated stiffness matrix of the elastic constants in the Cartesian coordinate system as shown below has characteristics of a fully general anisotropic material:

$$[C] = \begin{bmatrix} 447.1 & 60.4 & 199.1 & -35.3 & -33.1 & -43.5 \\ 60.4 & 531.1 & 61.0 & 18.7 & 7.5 & 86.7 \\ 199.1 & 61.0 & 509.6 & 57.9 & 31.5 & -39.4 \\ -35.3 & 18.7 & 57.9 & 176.6 & -36.5 & 12.0 \\ -33.1 & 7.5 & 31.5 & -36.5 & 294.6 & -3.8 \\ -43.5 & 86.7 & -39.4 & 12.0 & -3.8 & 127.7 \end{bmatrix} \text{GPa}. \tag{35}$$

The numerical values of the six independent Green's functions are obtained for an arbitrarily chosen field point with the spherical coordinates (r=2.0, θ=π/5, ϕ=π/6).

They are computed directly from Ting & Lee's (1997) exact solution using the formulations of Approach 1 (or Approach 2) and the present revised Fourier series scheme for increasing values of α in Eq. (19). The numerical values obtained are listed in Table 1 for up to 6 significant decimal digits. Excellent accuracy of the results from the present scheme is achieved even with α = 12, the *percentage errors* being of the order of 10^{-2}; with increasing values of α, the percentage errors decrease very quickly and are generally of the order of 10^{-4} when α = 20. The computed values of the first and second derivatives of **U** at this sample point using the re-formulated Fourier series scheme with α = 20 are listed in Tables 2 and 3, respectively. Also shown are the corresponding exact solutions. As can be seen, the accuracy of the numerical evaluations of these quantities achieved using the Fourier series approach remains excellent indeed. It should be mentioned that the calculations in the Fourier series scheme have been carried out with double precision arithmetic. Although this is not really necessary, the rate of convergence of the results with α has been found from some limited numerical experiments to be somewhat better than with single precision arithmetic. Also, this rate of convergence of the different components of the Green function derivatives in particular would obviously not be uniform in general as it depends very much on the degree of anisotropy, i.e. on how rapidly the material properties change with the orientation of the different coordinate directions. In any case, it should also be remarked that mechanical properties of materials are typically given with only 3 or 4 significant figures in accuracy. Thus, the very small percentage errors seen in these tables for the results of **U**, $\mathbf{U}^{'}$ and $\mathbf{U}^{''}$ are more than acceptable for engineering analysis.

To demonstrate the veracity of the perturbation scheme to resolve the numerical singularity problem in some of the derivatives of **U** when the load and field point both lie on the x_3-axis, the sample field point (0, 0, 2) is chosen. As discussed in Section 3, the perturbation of the spherical angle ϕ is carried out for the first derivatives by setting ϕ=10^{-6}, and θ=0 for $U_{ij,1}$ and $U_{ij,3}$; and θ=π/2 for $U_{ij,2}$. This is similarly done for the second derivatives, with ϕ=10^{-6}, the angle θ is set as θ=0 for $U_{ij,11}$ and $U_{ij,13}$; and θ=π/2 for $U_{ij,22}$ and $U_{ij,23}$. For $U_{ij,12}$, the coordinate transformation with Eq. (32-33) is employed. The computed results of $\mathbf{U}^{'}$ and $\mathbf{U}^{''}$ using the Fourier series scheme for this special case are shown in Tables 4 and 5, respectively, together with the corresponding exact solution. The percentage errors are, again, very small indeed.

Finally, the relative computational efficiency of the present re-formulated Fourier series scheme is compared to the original scheme proposed by the authors in Shiah *et al* (2012). To this end, the CPU times for evaluating **U, U'** and **U''** altogether, with α = 20, for increasing number of field points *N*using a PC with a quad-core Intel processor are recorded; they are compared to those reported in the paper. *N*

Table 1: Computed values of the Green's function U_{ij} (10^{-12}m) at r=2.0, θ=π/5, ϕ=π/6

U_{ij}	Ting & Lee	Fourier series	$\alpha = 12$	$\alpha = 14$	$\alpha = 16$	$\alpha = 18$	$\alpha = 20$
U_{11}	0.193135	Series Sum	0.193121	0.193127	0.193134	0.193135	0.193135
		(|%Diff.|)	(0.007%)	(0.004%)	(0.001%)	(0.000%)	(0.000%)
U_{12}	-0.009009	Series Sum	-0.009004	-0.009010	-0.009008	-0.009009	-0.009009
		(|%Diff.|)	(0.056%)	(0.011%)	(0.011%)	(0.000%)	(0.000%)
U_{13}	0.038025	Series Sum	0.037996	0.038019	0.038023	0.038025	0.038025
		(|%Diff.|)	(0.076%)	(0.016%)	(0.005%)	(0.000%)	(0.000%)
U_{22}	0.167744	Series Sum	0.167747	0.167743	0.167744	0.167744	0.167744
		(|%Diff.|)	(0.002%)	(0.001%)	(0.000%)	(0.000%)	(0.000%)
U_{23}	-0.006888	Series Sum	-0.006892	-0.006887	-0.006888	-0.006888	-0.006888
		(|%Diff.|)	(0.058%)	(0.015%)	(0.000%)	(0.000%)	(0.000%)
U_{33}	0.209534	Series Sum	0.209509	0.209525	0.209532	0.209533	0.209534
		(|%Diff.|)	(0.012%)	(0.004%)	(0.001%)	(0.000%)	(0.000%)

Table 2: Computed 1^{st} order derivatives of U_{ij} (10^{-12}) at a sample field point (2.0, π/5, π/6).

$U_{ij,l}$	Approach 1, 2	Fourier Series	|%Diff.|	$U_{ij,l}$	Approach 1, 2	Fourier Series	|%Diff.|
$U_{11,1}$	-0.027079	-0.027079	0.000%	$U_{22,1}$	-0.044581	-0.044581	0.000%
$U_{11,2}$	-0.058920	-0.058918	0.003%	$U_{22,2}$	0.000658	0.000658	0.000%
$U_{11,3}$	-0.078864	-0.078864	0.000%	$U_{22,3}$	-0.076247	-0.076247	0.000%
$U_{12,1}$	-0.011159	-0.011159	0.000%	$U_{23,1}$	-0.021226	-0.021227	0.005%
$U_{12,2}$	0.019726	0.019725	0.005%	$U_{23,2}$	0.024888	0.024888	0.000%
$U_{12,3}$	0.003719	0.003719	0.000%	$U_{23,3}$	0.005445	0.005445	0.000%
$U_{13,1}$	0.019569	0.019570	0.005%	$U_{33,1}$	-0.043524	-0.043522	0.005%
$U_{13,2}$	-0.049041	-0.049038	0.006%	$U_{33,2}$	-0.051609	-0.051604	0.010%
$U_{13,3}$	-0.014452	-0.014453	0.007%	$U_{33,3}$	-0.083131	-0.083134	0.004%

was varied from N = 5 to N = 10^6 and the CPU processing times are listed on Table 6. When normalized with respect to the corresponding times using Approach 1, the rate of decrease in the relative CPU time with increasing value of N, when using the Fourier series schemes, is illustrated in Fig. 3; in the figure, Fourier 1 and Fourier 2 refer to the original and re-formulated schemes, respectively. It can be seen from these results that when N = 10^6, the re-formulated Fourier series scheme takes only about 35% of the CPU time of that using the original Fourier series scheme which is already 3 times faster than Approach 1 to perform the same tasks.

Some qualifying remarks should perhaps be made about these enhanced performance numbers of both Fourier series schemes, however. In the case of BEM analysis based on the displacement-BIE, the second-order derivatives, $\mathbf{U}^{"}$, are only calculated if and when interior point stress solutions are required. Even then, they would typically be required for a very limited number of interior points. Thus, $\mathbf{U}^{"}$

Table 3: Computed 2^{nd} order derivatives of U_{ij} (10^{-12}) at a sample field point (2.0, $\pi/5$, $\pi/6$).

$U_{ij,lk}$	Approach 1,2	Fourier Series	|%Diff.|	$U_{ij,lk}$	Approach 1,2	Fourier Series	|%Diff.|
$U_{11,11}$	-0.037976	-0.037966	0.026%	$U_{22,11}$	-0.013541	-0.013542	0.007%
$U_{11,12}$	-0.010723	-0.010715	0.075%	$U_{22,12}$	0.000625	0.000624	0.160%
$U_{11,13}$	0.052645	0.052637	0.015%	$U_{22,13}$	0.057590	0.057591	0.002%
$U_{11,22}$	-0.008117	-0.008123	0.074%	$U_{22,22}$	-0.004864	-0.004870	0.123%
$U_{11,23}$	0.075798	0.075794	0.005%	$U_{22,23}$	0.000599	0.000601	0.334%
$U_{11,33}$	0.040751	0.040757	0.015%	$U_{22,33}$	0.060940	0.060939	0.002%
$U_{12,11}$	-0.002100	-0.002100	0.000%	$U_{23,11}$	0.014032	0.014033	0.007%
$U_{12,12}$	0.008214	0.008215	0.012%	$U_{23,12}$	0.001968	0.001970	0.102%
$U_{12,13}$	0.011078	0.011078	0.000%	$U_{23,13}$	0.017288	0.017287	0.006%
$U_{12,22}$	-0.015174	-0.015177	0.020%	$U_{23,22}$	-0.027170	-0.027161	0.033%
$U_{12,23}$	-0.021465	-0.021463	0.009%	$U_{23,23}$	-0.020437	-0.020441	0.020%
$U_{12,33}$	-0.002184	-0.002185	0.046%	$U_{23,33}$	-0.007427	-0.007426	0.013%
$U_{13,11}$	-0.078767	-0.078753	0.018%	$U_{33,11}$	-0.070616	-0.070599	0.024%
$U_{13,12}$	-0.023311	-0.023302	0.039%	$U_{33,12}$	-0.017369	-0.017364	0.029%
$U_{13,13}$	0.022105	0.022094	0.050%	$U_{33,13}$	0.089135	0.089123	0.013%
$U_{13,22}$	0.019411	0.019411	0.000%	$U_{33,22}$	-0.063196	-0.063217	0.033%
$U_{13,23}$	0.060930	0.060921	0.015%	$U_{33,23}$	0.089151	0.089151	0.000%
$U_{13,33}$	-0.014315	-0.014305	0.070%	$U_{33,33}$	0.024104	0.024113	0.037%

Table 4: Computed 1^{st} order derivatives of U_{ij} (10^{-12}) at field point (0, 0, 2).

$U_{ij,l}$	Approach 1,2	Fourier Series	|%Diff.|	$U_{ij,l}$	Approach 1,2	Fourier Series	|%Diff.|
$U_{11,1}$	-0.001469	-0.001466	0.204%	$U_{22,1}$	0.000966	0.000967	0.104%
$U_{11,2}$	0.004723	0.004723	0.000%	$U_{22,2}$	0.002815	0.002815	0.000%
$U_{11,3}$	-0.095345	-0.095345	0.000%	$U_{22,3}$	-0.081803	-0.081803	0.000%
$U_{12,1}$	-0.007406	-0.007404	0.027%	$U_{23,1}$	-0.013368	-0.013368	0.000%
$U_{12,2}$	0.002116	0.002115	0.047%	$U_{23,2}$	0.016962	0.016962	0.000%
$U_{12,3}$	0.003751	0.003751	0.000%	$U_{23,3}$	0.001652	0.001652	0.000%
$U_{13,1}$	0.058453	0.058439	0.024%	$U_{33,1}$	0.022486	0.022480	0.027%
$U_{13,2}$	-0.011015	-0.011015	0.000%	$U_{33,2}$	0.040571	0.040571	0.000%
$U_{13,3}$	-0.003579	-0.003579	0.000%	$U_{33,3}$	-0.089485	-0.089485	0.000%

is not calculated simultaneously at every field point of the boundary elements unlike $\mathbf{U}$ and $\mathbf{U}^{'}$. In practice therefore, the savings in CPU time of the Fourier series scheme, although still significant, may not be as dramatic as is shown here when, say, $\alpha = 20$ is employed. On the other hand, it is also evident from Table 1 that even with lower values of α, the accuracy of the computed Green function values is still highly acceptable for practical engineering analysis. This will reduce the computer processing time further as there will be even fewer terms in the series summation.

Table 5: Computed 2^{nd} order derivatives of U_{ij} (10^{-12}) at the field point (0, 0, 2).

$U_{ij,lk}$	Approach 1, 2	Fourier Series	|%Diff.|	$U_{ij,lk}$	Approach 1, 2	Fourier Series	|%Diff.|
$U_{11,11}$	0.014164	0.014149	0.106%	$U_{22,11}$	-0.063683	-0.063693	0.016%
$U_{11,12}$	0.000616	0.000628	1.948%	$U_{22,12}$	-0.003897	-0.003873	0.616%
$U_{11,13}$	0.001469	0.001466	0.204%	$U_{22,13}$	-0.000966	-0.000967	0.104%
$U_{11,22}$	-0.082170	-0.082172	0.002%	$U_{22,22}$	-0.011774	-0.011772	0.017%
$U_{11,23}$	-0.004723	-0.004723	0.000%	$U_{22,23}$	-0.002815	-0.002815	0.000%
$U_{11,33}$	0.095345	0.095345	0.000%	$U_{22,33}$	0.081803	0.081803	0.000%
$U_{12,11}$	-0.014477	-0.014446	0.214%	$U_{23,11}$	-0.022131	-0.022119	0.054%
$U_{12,12}$	0.010444	0.010442	0.019%	$U_{23,12}$	-0.017284	-0.017299	0.087%
$U_{12,13}$	0.007406	0.007404	0.027%	$U_{23,13}$	0.013368	0.013368	0.000%
$U_{12,22}$	0.011114	0.011115	0.009%	$U_{23,22}$	0.005416	0.005416	0.000%
$U_{12,23}$	-0.002116	-0.002115	0.047%	$U_{23,23}$	-0.016962	-0.016962	0.000%
$U_{12,33}$	-0.003751	-0.003751	0.000%	$U_{23,33}$	-0.001652	-0.001652	0.000%
$U_{13,11}$	0.004743	0.004657	1.813%	$U_{33,11}$	0.005989	0.005996	0.117%
$U_{13,12}$	-0.002212	-0.002201	0.497%	$U_{33,12}$	-0.008724	-0.008720	0.046%
$U_{13,13}$	-0.058453	-0.058439	0.024%	$U_{33,13}$	-0.022486	-0.022480	0.027%
$U_{13,22}$	-0.015159	-0.015158	0.007%	$U_{33,22}$	-0.037554	-0.037553	0.003%
$U_{13,23}$	0.011015	0.011015	0.000%	$U_{33,23}$	-0.040571	-0.040571	0.000%
$U_{13,33}$	0.003579	0.003579	0.000%	$U_{33,33}$	0.089485	0.089485	0.000%

Table 6: CPU-times for computing **U,** $\mathbf{U}^{'}$ and $\mathbf{U}^{"}$ with increasing number of field points, N.

N	Approach 1 (Seconds)	Fourier 1 (Seconds)	Fourier 2 (Seconds)
5	0.0156	0.7500	0.4056
10	0.0156	0.7600	0.4056
50	0.0312	0.7800	0.4056
10^2	0.0624	0.7800	0.4056
5×10^2	0.2800	0.8400	0.4212
10^3	0.5800	0.9400	0.4524
5×10^3	2.8900	1.6700	0.7176
10^4	5.7700	2.5400	1.0452
5×10^4	28.7000	9.7500	3.5880
10^5	57.4600	18.7200	6.7704
5×10^5	286.6400	90.7100	32.1986
10^6	573.4800	180.6500	63.9604

5 Conclusions

A double Fourier series representation of Ting and Lee's (1997) explicit, real variable, algebraic form fundamental solution for 3D anisotropic elasticity was reported

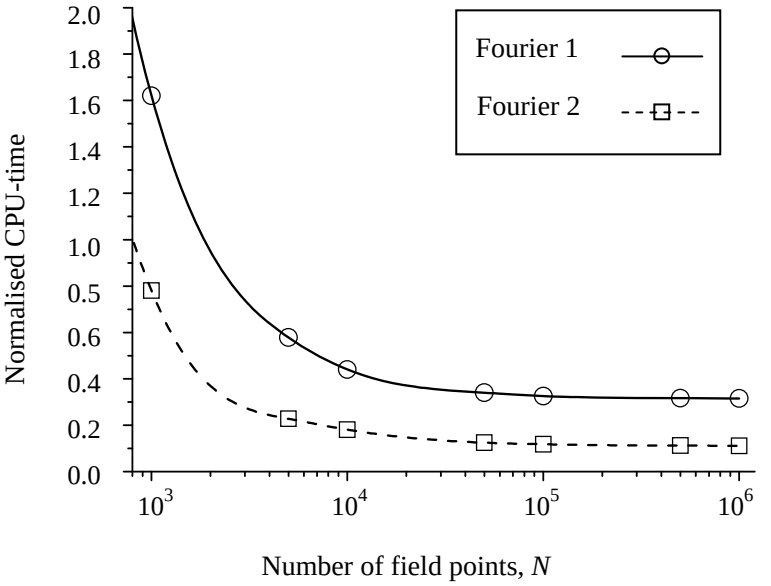

Figure 3: Variation of CPU time, normalized with respect to that using Approach 1, for computing **U,** $\mathbf{U}^{'}$ and $\mathbf{U}^{''}$ together with increasing number of field points, N.

by the present authors very recently. Derivatives of the fundamental solution can also be obtained from direct spatial differentiation on the Fourier series via the chain rule. It was shown to offer considerable savings in the computational effort for the numerically evaluation of the Green's function and its derivatives without any significant loss in accuracy. In addition, it is even simpler to implement into a BEM code due to the less elaborate formulation. The better computational efficiency stems primarily from the fact that the Fourier coefficients need to be evaluated only once and is independent of the number of field points in the problem.

In this study, advantage has been taken of some features of the coefficients Fourier series, and upon re-arrangement and further simplification of the series. In doing so, the total number of terms that need to be calculated in the series summations has been drastically reduced. This has enhanced the efficiency of the Fourier series scheme to compute the fundamental solution and its derivatives for 3D general anisotropy. The efficacy of this re-formulated scheme has been demonstrated with some examples. Ways to overcome some numerical singularity problems, should they occur have also been described and verified by an example. With computations of the fundamental solution and its derivatives required at every field point in a BEM analysis, this scheme offers an even more attractive alternative to the direct

evaluation of their exact analytical forms.

Acknowledgement: The authors gratefully acknowledge the financial support from the National Science and Engineering Research Council of Canada and the National Science Council of Taiwan (NSC 99-2221-E-035-027-MY3).

References

Barnett, D.M. (1972): The precise evaluation of derivatives of the anisotropic elastic Green's function. *Phy. Stat. Solid (b)*, 49, 741-748.

Buroni, F.C.; Saez, A. (2010): Three-dimensional Green's function and its derivative for materials with general anisotropic magneto-electro-elastic coupling. *Proc. Royal Soc. A*, 466, 515-537.

Gray, L.J.; Gosh, D.; Kaplan, T. (1996): Evaluation of the anisotropic Green's function in three-dimensional elasticity. *Comput. Mech.*, 17, 253-261.

Huntington, H.B. (1958): *The Elastic Constants of Crystal*. Academic Press, New York.

Lee,V.G. (2003): Explicit expression of derivatives of elastic Green's functions for general anisotropic materials. *Mech. Res. Comm.*, 30, 241–249.

Lee,V.G. (2009): Derivatives of the three-dimensional Green's function for anisotropic materials. *Int. J. Solids Struct., 46, 1471-1479.*

Lifshitz, I.M.; Rozenzweig, **L.N.** (1947): Construction of the Green tensor for the fundamental equation of elasticity theory in the case of unbounded elastically anisotropic medium, *Zh. Eksp. Teor. Fiz.*, 17, 783-791.

Phan, P.V.; Gray, L.J.; Kaplan, T. (2004): On the residue calculus evaluation of the 3D anisotropic elastic Green's function. *Comm. Numer. Methods Engng.*, 20, 335-341.

Sales, M.A.; Gray, L.J. (1998): Evaluation of the anisotropic Green's function and its derivatives. *Comp. & Struct.*, 69, 247-254.

Schclar, N.A. (1994): *Anisotropic Analysis Using Boundary Elements*. Computational Mechanics Pub., U.K.

Shiah, Y.C.; Tan, C.L.; Lee, V.G.; Chen, Y.H. (2008a): Evaluation of Green's functions for 3D anisotropic elastic solids. *Advances in Boundary Element Techniques IX*, *Proc. BeTeq 2008 Conf.*, *Seville*, R. Abascal & M.H. Aliabadi (eds.), E.C. Ltd. (U.K.), pp. 119-124.

Shiah, Y.C.; Tan, C.L.; Lee, V.G. (2008b): Evaluation of explicit-form fundamental solutions for displacements and stresses in 3D anisotropic elastic solids. *CMES: Computer Modeling in Engineering & Sciences*, 34, 205-226.

Shiah, Y.C.; Tan, C.L.; Sun, W.X.; Chen, Y.H. (2010): On the displacement derivatives of the three-dimensional Green's function for generally anisotropic bodies. *Advances in Boundary Element Techniques XI*, *Proc. BeTeq 2010 Conf.*, *Berlin*, Ch. Zhang, M.H. Aliabadi & M. Schanz (eds.), E.C. Ltd. (U.K.), pp. 426-432.

Shiah, Y.C.; Tan, C.L.; Lee, R.F. (2010): Internal point solutions for displacements and stresses in 3D anisotropic elastic solids using the boundary element method. *CMES: Computer Modeling in Engineering & Sciences*, 69, 167-197.

Shiah, Y.C.; Tan, C.L. (2011): Higher order Green's function derivatives and BEM evaluation of stresses at interior points in a 3D generally anisotropic solid. *Advances in Boundary Element Techniques XII, Proc. Beteq 2011 Conf., Brasilia*, E.I. Albuquerque & M.H. Aliabadi (eds.), E.C. Ltd (U.K.), pp. 336-342.

Shiah, Y.C.; Tan, C.L.; Wang, C.Y. (2012): Efficient computation of the Green's function and its derivatives for three-dimensional anisotropic elasticity in BEM analysis. *Engng. Analysis Boundary Elem.*, 6936, 1746-1755.

Tan, C.L.; Shiah, Y.C.; Lin, C.W. (2009): Stress analysis of 3D generally anisotropic elastic solids using the boundary element method. *CMES: Computer Modeling in Engineering & Sciences*, 41, 195-214.

Tavara, L.; Ortiz, J.E; Mantic, V.; Paris, R. (2008): Unique real-variable expressions of displacement and traction fundamental solutions covering all transversely isotropic materials for 3D BEM. *Int. J. Numer. Methods Engng.*, 74, 776-798.

Ting, T.C.T.; Lee,V.G. (1997):The three-dimensional elastostic Green's function for general anisotropic linear elastic solid. *Q. J. Mech. Appl. Math.*, 50, 407-426.

Tonon, F.; Pan, E.; Amadei, B. (2001): Green's functions and boundary element method formulation for 3D anisotropic media. *Comp. & Struct.*, 79, 469-482.

Wang, C.Y. (1997): Elastic fields produced by a point source in solids of general anisotropy. *J. Engng. Math.*, 32, 41-52.

Wang, C.Y.; Denda, M. (2007): 3D BEM for general anisotropic elasticity. *Int. J. Solids Struct.*, 44, 7073-7091.

Wilson, R.B.; Cruse, T.A. (1978): Efficient implementation of anisotropic three dimensional boundary integral equation stress analysis. *Int. J. Numer. Methods Engng.*, 12, 1383-1397.